ORIGINAL RESEARCH

Percentage Signal Recovery Derived from MR Dynamic Susceptibility Contrast Imaging Is Useful to Differentiate Common Enhancing Malignant Lesions of the Brain

R. Mangla
B. Kolar
T. Zhu
J. Zhong
J. Almast
S. Ekholm

BACKGROUND AND PURPOSE: Differentiation of enhancing malignant lesions on conventional MR imaging can be difficult and various newer imaging techniques have been suggested. Our aim was to evaluate the role of PSR obtained from DSC perfusion measurements in differentiating lymphoma, GBM, and metastases. The effectiveness of PSR was compared with that of rCBV. We hypothesized that the newly defined parameter of PSR is more sensitive and specific in differentiating these lesions.

MATERIALS AND METHODS: This retrospective study included 66 patients (39 men and 27 women; age range: 27–82 years) with a pathologically proved diagnosis of primary CNS lymphoma, GBM, or metastases (22 patients in each group). Mean PSR, min PSR, max PSR, and rCBV were calculated. The classification accuracy of these parameters was investigated by using ROC.

RESULTS: Mean PSR was high (113.15 ± 41.59) in lymphoma, intermediate in GBM (78.22 ± 14.27), and low in metastases (53.46 ± 12.87) with a P value < .000. F values obtained from 1-way ANOVA analysis for mean, min, and max PSR ratios were 29.9, 39.4, and 23.4, respectively, which were better than those of rCBV (11.1) in differentiating the 3 groups. Max PSR yielded the best ROC characteristics with an A_z of 0.934 (95% CI, 0.877–0.99) in differentiating lymphoma from metastases and GBM. The A_z for mean and min PSR of 0.938 (95% CI, 0.0.884–0.990) and 0.938 (95% CI, 0.884–0.991), respectively, was better than rCBV (A_z, 0.534; 95% CI, 0.391–0.676) in the differentiation of metastases from GBM and lymphoma ($P \leq .0001$).

CONCLUSIONS: PSR appears to be a parameter that helps in differentiating intracerebral malignant lesions such as GBM, metastases, and lymphoma.

ABBREVIATIONS: ANOVA = analysis of variance; A_z = area under the curve; BBB = blood-brain barrier; CI = confidence interval; CNS = central nervous system; DSC = dynamic susceptibility-weighted contrast-enhanced; EES = extravascular/extracellular space; FLAIR = fluid-attenuated inversion recovery; FSE = fast spin-echo; GBM = glioblastoma multiforme; max = maximum; min = minimum; PSR = percentage of signal-intensity recovery; rCBV = relative cerebral blood volume; ROC = receiver operating characteristic analysis

The characterization and differentiation of intracranial malignant lesions, such as gliomas, metastases, and lymphoma can be challenging, and there is considerable overlap in their imaging features. The differentiation of these enhancing malignant lesions is often required because management can differ substantially, depending on the type of lesion. There are studies that have looked into the role of the newer imaging techniques in the differentiation of these lesions. Diffusion and rCBV measurements with perfusion-weighted sequences have highlighted some salient features in these lesions but are not always confirmatory.[1-3]

DSC MR perfusion imaging has been used to assess the status of the capillaries and microvessel attenuation of these tumors. Changes in rCBV maps, which reflect the microvessel attenuation, are markers of neoangiogenesis taking place within the lesion, and rCBV has become one of the most important hemodynamic variables used in the characterization of tumors. It has been suggested that rCBV is considerably higher in glioblastomas, and it has been used in the grading of gliomas.[4] In lymphomas, rCBV has been shown to be lower than in gliomas and metastases; this difference can be attributed to the lack of neoangiogenesis.[5] However, with regard to gliomas and metastases, there is an overlap in rCBV values because both have high rCBV; PSR has been reported to be a better criterion than rCBV for differentiating these lesions.[6]

PSR, as the name implies, represents the percentage of signal intensity that is recovered at the end of the first pass of contrast agent, relative to baseline (the signal intensity before administration of contrast). There is an initial drop in signal intensity after administration of the contrast agent, which, after the first pass, returns toward the baseline. The degree of this recovery is dependent on many factors related to contrast agent leakage, the size of extravascular space, and the rate of blood flow.

There are reports of significantly reduced PSR in metastatic lesions, compared with GBM.[6] The latter has been reported to have a lower recovery of signal intensity than primary CNS lymphoma. The recovery curve in lymphomas can go above the baseline (overshooting).[7,8] This hemodynamic variable not only has the potential to differentiate these lesions but also

Received August 17, 2010; accepted after revision October 18.

From the Department of Imaging Sciences, University of Rochester, Rochester, New York.

Please address correspondence to Rajiv Mangla MD, Department of Imaging Sciences, PO Box 648, University of Rochester School of Medicine and Dentistry, 601 Elmwood Ave, Rochester, NY 14642; e-mail: rajiv_mangla@urmc.rochester.edu

DOI 10.3174/ajnr.A2441

has another important advantage, as noted by Cha et al,[6] of relative ease in quantification on a workstation without the need for sophisticated software packages.

We have performed a retrospective study of common malignant intracranial lesions to evaluate the diagnostic role of DSC imaging in enhancing and perienhancing regions, by using rCBV and PSR measurements. The aim was to identify the value of PSR in the differentiation of these lesions. We also wanted to investigate the classification accuracy of these parameters by using ROC.

Materials and Methods

This retrospective study group included all 26 cases of primary CNS lymphoma, from January 2003 to July 2009 in our hospital, for which perfusion imaging was available. We excluded 4 patients: Two had significant artifacts in the perfusion data, 1 patient had only leptomeningeal disease, and 1 patient was immunocompromised. This left us with 22 cases of biopsy-proved primary CNS lymphomas in nonimmunocompromised patients with optimum DSC imaging. We also included the first 22 consecutive cases of histologically proved GBM with optimum DSC image quality as well as 22 consecutive cases of solitary intracranial metastases from the same time period. Twelve of the metastases were biopsy-proved; and in the other 10, the diagnosis was based on known primary cancer. Among the 12 biopsied cases, 8 originated from the lung, 2 originated from the esophagus, and 1 was a melanoma from the skin. The primary tumor was unknown in 1 case but was presumed to be from the lung or thyroid based on the histopathologic features of the metastasis. The nonbiopsied cases had biopsy-proved primary lesions elsewhere, including 5 lung lesions and 1 each from the breast, thyroid, skin, kidney, and uterus. All patients were treatment-naïve; and only enhancing lesions were included in the study.

Imaging Protocol

Imaging was performed on a 1.5T Sigma LX scanner (GE Healthcare, Milwaukee, Wisconsin). Conventional sequences included axial T2 FLAIR, T1 FSE, gradient recalled-echo, T2 FSE, and postcontrast T1-weighted images in 3 planes. DSC imaging was performed by using a gradient-recalled T2*-weighted echo-planar imaging sequence. Parameters used were TR/TE = 1500/50 ms, flip angle = 80°, NEX = 1, matrix size = 128 × 96, and section thickness = 6 mm (with no gap). A total of 60 image volumes were acquired, in which the first 10 acquisitions were executed before starting the contrast agent injection to establish a precontrast baseline. At the end of the 10th image-volume acquisition, 0.15 mmol/kg of body weight gadopentetate dimeglumine was injected with a power injector at a rate of 5 mL/s through an 18- or 20-ga intravenous catheter. This was immediately followed by a bolus injection of saline (total of 20 mL at 5 mL/s). Twelve contiguous axial section levels were chosen for the analysis outlined in the next section, on the basis of lesion extent, as determined by the precontrast T2 FLAIR images. No contrast agent was administered before DSC perfusion MR imaging.

Postprocessing and Perfusion Measurements

rCBV Measurement. Postprocessing was conducted off-line by 1 of the authors, blinded at the time of analysis to the histologic data. The analysis was carried out with the Lund University Perfusion Evaluation software, which is written in Interactive Data Language (Research Systems, Boulder, Colorado), by using the extended BBB leakage correction as described by Haselhorst et al.[9] The T2 FLAIR, T2 FSE, and contrast-enhanced T1-weighted images were referenced during the calculation of rCBV. Regions of interest were drawn on the gray-scale perfusion maps overlaid on contrast-enhancing tumor on T1-weighted images by 2 authors (R.M. and B.K.) independently, each with >3 years of experience in neuroradiology and perfusion analysis. Multiple regions of interest of 30–40 mm^2 were placed over several hot spots, and the max rCBV of all regions of interest was chosen. This method has been described as having a better inter- and intraobserver agreement.[10] T1- and T2-weighted images and raw data of perfusion images were used to ensure that regions of interest did not include any hemorrhage or apparent blood vessels. Similarly, the region of interest with the max rCBV in the peritumoral or perienhancing region was selected. For normalization, another region of interest with a size of approximately 30–50 mm^2 was placed in the contralateral normal-appearing white matter, carefully excluding gray matter. The rCBV ratio was then obtained by dividing the lesion rCBV by the values obtained from the contralateral normal-appearing white matter.

PSR Measurement. For measurement of PSR, postprocessing was performed with the FuncTool 2 application software on a GE Healthcare workstation. Regions of interest were drawn on the gray-scale perfusion maps overlaid on contrast-enhancing tumor on T1-weighted images. A region of interest of 30–40 mm^2 was moved within the tumor area to look for the highest and lowest recoveries on T2*-weighted signal-intensity curves and was selected for max and min PSR, respectively. Another region of interest was placed over the entire contrast-enhancing portion of the lesion, excluding the nonenhancing necrotic area, to trace the mean PSR value. For normalization, a region of interest of approximately 30–50 mm^2 was also placed in the contralateral normal-appearing white matter, and ratios were obtained. The T2*-weighted signal-intensity curves obtained for these regions of interest were then analyzed. The PSR was calculated as described by Cha et al[6]:

$$PSR = 100\% \times (S_1 - S_{min})/(S_0 - S_{min}),$$

where S_1 is postcontrast T2*-weighted signal intensity; S_0 is precontrast T2*-weighted signal intensity, and S_{min} is min T2*-weighted signal intensity.

Statistical Analysis

The diagnostic accuracy of various perfusion parameters was analyzed by using SAS, Version 9.1 (SAS Institute, Cary, North Carolina) and the Statistical Package for the Social Sciences, Version 15.0 (SPSS, Chicago, Illinois) software. One-way ANOVA was performed, and analysis also included calculation of the *F*-statistic, which defines the ratio of the variance between groups to the variance within the group.[11] As *F* goes up, *P* goes down (ie, there is more confidence regarding a difference between 2 means).

ROC was also performed for various perfusion parameters in regard to their ability to differentiate lymphoma from metastases and GBM, and metastases from GBM and lymphoma. The A_z was obtained to determine which continuous variables (enhancing PSR, enhancing rCBV, perienhancing PSR, and perienhancing rCBV) were the most predictive for diagnosing metastases and lymphomas. The ROCs were performed on the basis of logistic regression models, with methods for differentiation as predictive variables. Because there is a trade-off between sensitivity and specificity in the selection of cutoff points, which are not intrinsic to the test, A_z was calculated. Differences in the A_z were tested for significance by using a bivariate χ^2 test.

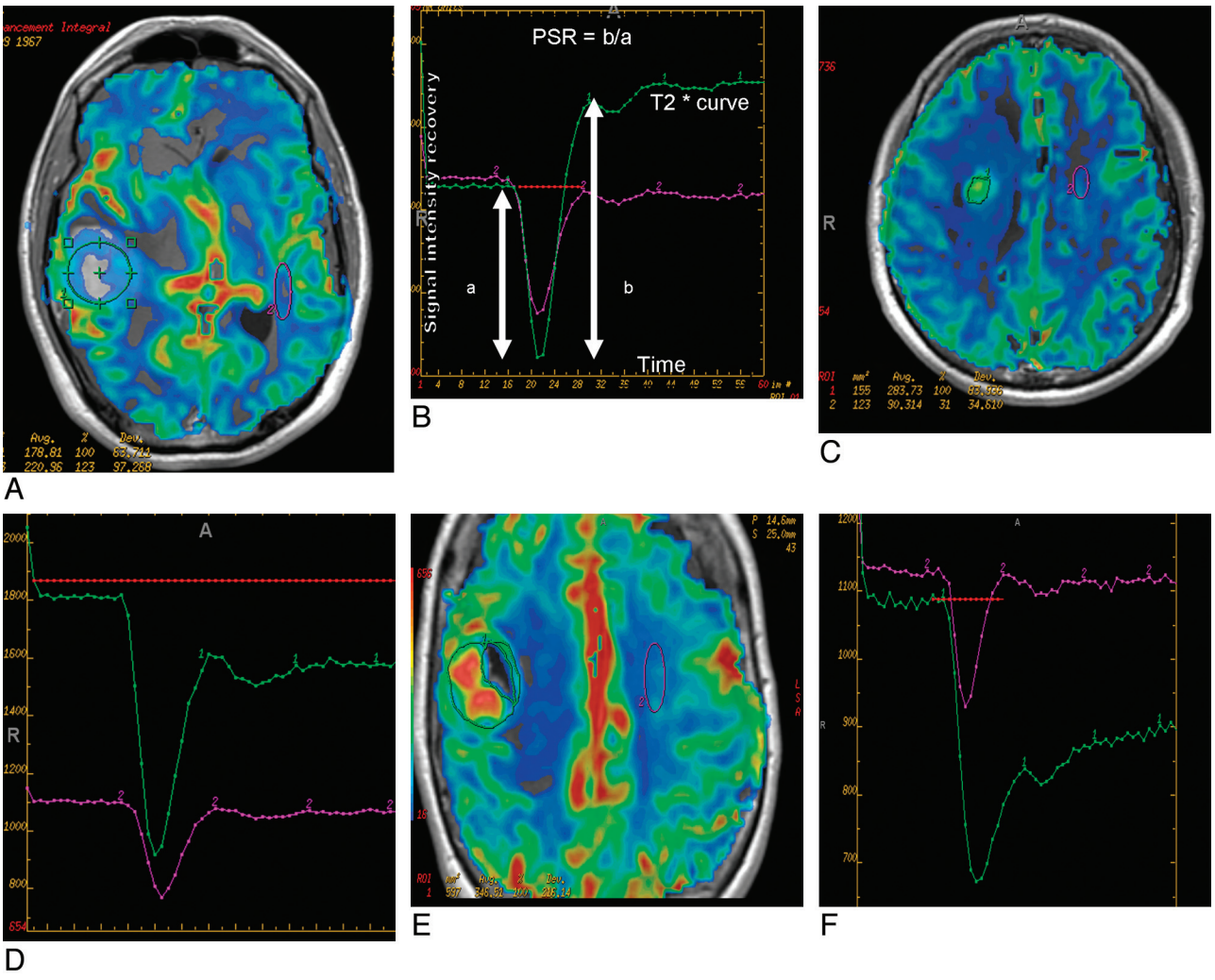

Fig 1. *A* and *B*, Perfusion maps overlaid on postcontrast T1-weighted image (*A*) in an enhancing mass lesion of the brain. The large green region of interest placed on the enhancing mass lesion to measure the mean signal-intensity recovery shows overshoot from baseline on the recovery maps (*B*). The lesion proved to be a lymphoma on histopathology. *C* and *D*, Perfusion maps overlaid on postcontrast T1-weighted image (*C*) in a mass lesion of the brain surrounded by significant edema, which proved to be GBM on histopathology. The large green region of interest placed on the enhancing mass lesion shows approximately 77% mean signal-intensity recovery on the recovery maps (*D*). *E* and *F*, Perfusion maps overlaid on postcontrast T1-weighted image (*E*) in an enhancing mass lesion of the brain. The large green region of interest placed on the enhancing mass lesion shows about 32% mean signal-intensity recovery on the recovery maps (*F*). The lesion proved to be a metastases on histopathology.

Results

Signal-intensity curves and rCBV maps in the 3 different groups of lesions showed characteristic features, including significant overshoot with high max and mean PSR in lymphomas (Fig 1*A*), high rCBV and intermediate PSR in gliomas (Fig 1*B*), and low mean PSR in metastatic lesions (Fig 1*C*).

One-way ANOVA of the mean and standard errors (Fig 2), derived for the various perfusion parameters, showed significant differences among the 3 groups for all parameters studied (Table 1). The *F*-statistic showed higher values for max, mean, and min PSR than rCBV.

A_z, obtained from ROC for various perfusion parameters in the differentiation of lymphoma from GBM and metastases, showed that max PSR had a higher A_z (0.933) compared with other parameters. Similarly, min and mean PSR had a higher A_z (0.938) compared with other parameters in differentiating metastases from GBM and lymphoma as measured in enhancing tumor (Table 2 and Fig 3).

Table 3 shows *P* values for differences in ROCs, tested for significance by using the bivariate χ^2 test. Mean PSR was superior to rCBV but equivalent to min PSR in differentiating metastases from GBM and lymphoma. Maximum PSR was better than rCBV in distinguishing lymphoma from GBM and metastases ($P < .01$). The mean PSR appeared to be a better criterion than rCBV, but the difference was not statistically significant.

Low rCBV and signal-intensity recovery in metastases compared with GBM and lymphoma in perienhancing regions was noted. The A_z was modest for rCBV at 0.79. The enhancing PSR was distinctively better, with an A_z of 0.93 (Fig 3*C*).

Table 4 shows the sensitivity and specificity of PSR in differentiating these lesions. In our study, the max PSR was very helpful in the differentiation of lymphoma from GBM and metastases with an optimum cutoff of 1.14, which showed 82% and 93% sensitivity and specificity, respectively. The min PSR was helpful in differentiating metastases from glioblastoma and lymphoma, with an optimum cutoff of <0.51, which showed 86% and 89% sensitivity. Max PSR of >136% and min PSR of <40% were 100% specific for diagnosis of lymphoma and metastases respectively.

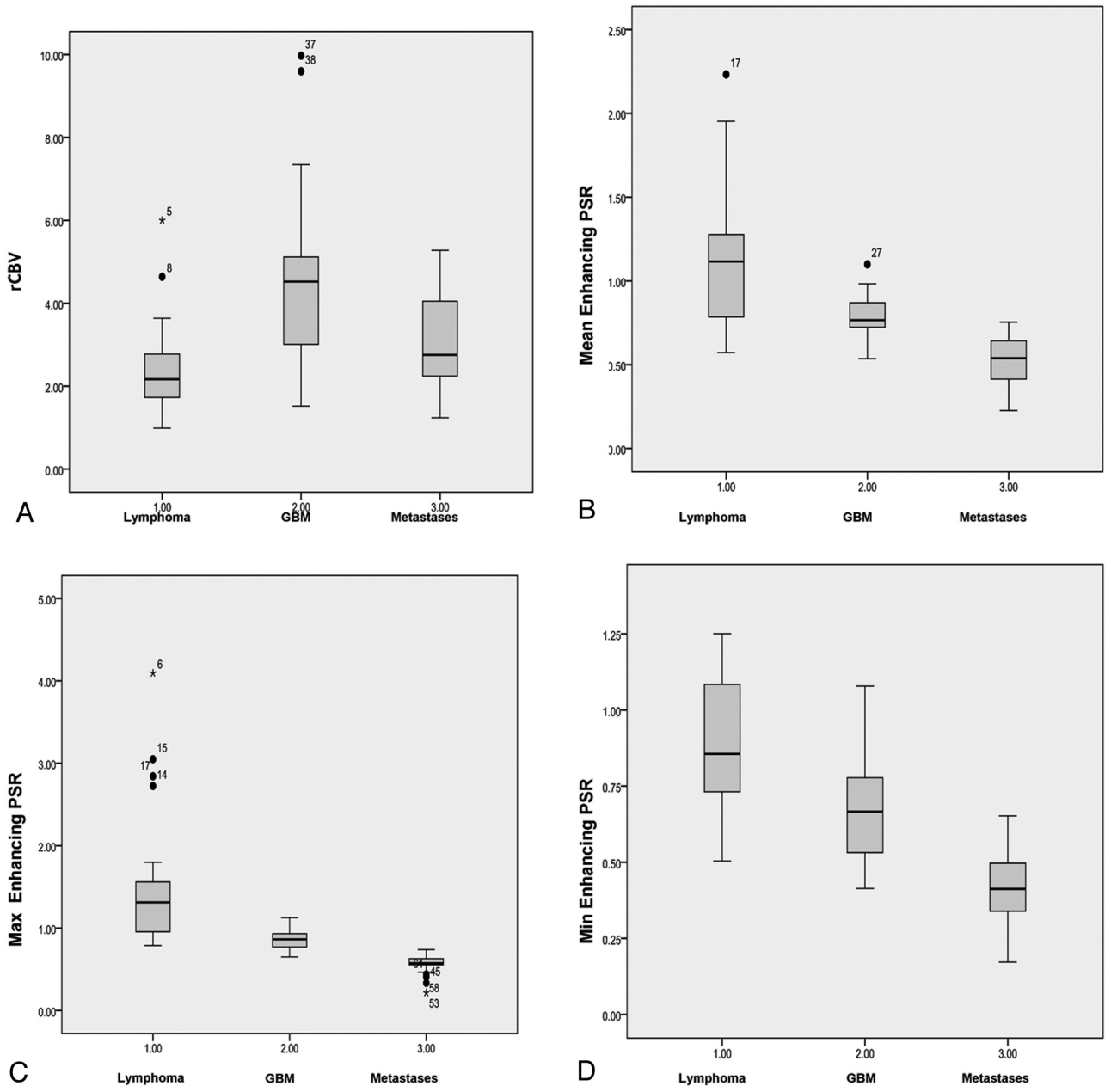

Fig 2. Boxplots showing various perfusion parameters like rCBV (*A*), mean PSR (*B*), max PSR (*C*), and min PSR (*D*) in differentiating lymphoma, GBM, and metastases.

Table 1: Mean values and SDs of perfusion parameters in differentiating malignant lesions of the brain

	Contrast-Enhancing Lesion				Perienhancing Lesion	
	rCBV	Mean PSR Ratio	Max PSR Ratio	Min PSR Ratio	rCBV	Mean PSR Ratio
Lymphoma	2.43 ± 1.19	113.15 ± 41.59	158.86 ± 87.06	89.57 ± 23.63	0.87 ± 0.17	99.80 ± 25.33
GBM	4.72 ± 2.19	78.22 ± 14.27	87.06 ± 13.16	66.04 ± 16.24	1.39 ± 0.51	93.00 ± 10.50
Metastases	2.93 ± 1.18	53.46 ± 12.87	55.76 ± 12.56	41.82 ± 12.95	0.48 ± 0.26	80.97 ± 8
P value lymphoma from GBM	.000	.001	.000	.015	.002	.16
P value GBM vs metastases	.021	.000	.000	.000	.001	.000
F (ANOVA)	>11.1	>29.9	>23.4	>39.3	>18.4	>7.2

Discussion

An intracranial contrast-enhancing lesion can have many different etiologies, including malignant lesions such as GBM; metastases and lymphoma; and nonneoplastic lesions like subacute infarcts, tumefactive demyelinating lesions, and various infective lesions. Our study illustrates the utility of signal-intensity recovery in a DSC measurement for differentiating the common enhancing malignant lesions of the brain. PSR calculation from the T2* signal-intensity curve is not labor-intensive and does not require elaborate postprocessing but

Table 2: A_z for various parameters

	Enhancing Lesion				Perienhancing Lesion	
	rCBV	Mean PSR	Max PSR	Min PSR	rCBV	PSR
Lymphoma from GBM and metastases	.759 (.634–.884)	.880 (.789–.970)	.933 (.877–.990)	.909 (.828–.990)	.608 (.461–.756)	.658 (.494–.822)
Metastases from GBM and lymphoma	.534 (.391–.676)	.938 (0.884–0.990)	.928 (0.824–0.973)	.938 (.884–.991)	.798 (.662–.929)	.849 (.737–.961)

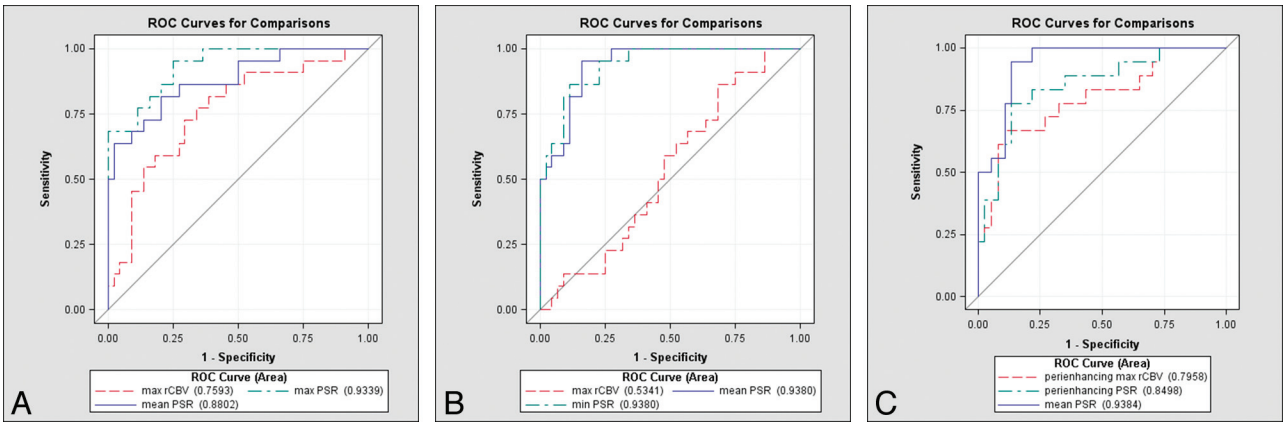

Fig 3. *A*, ROC for comparison of mean PSR, max PSR, and max rCBV in an enhancing lesion for differentiation of lymphoma from GBM and metastases. *B*, ROC for comparison of mean PSR, min PSR, and max rCBV in an enhancing lesion in differentiating metastases from GBM and lymphoma. *C*, ROC for comparison of mean PSR in an enhancing lesion and PSR and max rCBV in the peritumoral region.

Table 3: *P* values for differences in ROC curves[a]

	Comparison	χ^2	*P* Value
Differentiation of metastases from GBM and lymphoma	Mean PSR vs rCBV	24.1782	<.0001
	Minimum PSR vs mean PSR	0.0000	1.0000
Differentiation of lymphoma from GBM and metastases	Maximum PSR vs rCBV	6.4777	<.011
	Maximum PSR vs mean PSR	3.3210	.0684

[a] Tested for significance using the bivariate χ^2 test.

Table 4: Decision thresholds

	Threshold	Sensitivity	Specificity
Max PSR % in lymphoma from other	>94	100	69
	>114	82	93
	>136	72	100
Mean PSR % in lymphoma from other	>70	100	34
	>120	59	100
	>103	78	94
Mean PSR % in metastases from other	<40	.50	100
	<75	100	83
	<67	95	85
Min PSR % in metastases from other	<40	.50	100
	<72	100	81
	<51	86	89

appears to be effective in eliciting distinctive characteristics, which helps in differentiating these lesions. The high max PSR (overshoot from baseline) was very suggestive of lymphoma, and a low mean PSR appears to be indicative of metastases. The results of this study also show that PSR is a robust parameter, which can help in differentiating intracerebral malignant lesions, such as GBM, metastases, and lymphoma, and may aid in the management of these malignant tumors of the brain.

Although there is a considerable overlap in the MR imaging features for some of the more common intracranial malignant lesions, such as GBM, metastases, and lymphoma, histologic studies have shown considerable differences in the structure of the tumor capillaries in these lesions.[12] The capillaries noted in GBM are characterized by various features, including glomeruloid capillaries, simple vascular hyperplasia, and delicate neocapillaries as well as BBB disruption. However, capillaries in metastatic lesions are similar in their structure to those from the site of the primary systemic cancer and have no similarity to normal brain capillaries. They also have prominent capillary fenestration and complete lack of BBB components.[13] Lymphomas, on the other hand, have characteristic histopathologic features with angiocentric growth patterns. The tumor cells of lymphomas form multiple thick layers around the host vessels, and there is also an associated widening of the perivascular space. Neovascularization is not a prominent feature, though vascular abnormalities such as tumor invasion of endothelial cells and even into the vessel lumen is often seen. These vascular differences are also the origin of the variability in perfusion, which can help in the differentiation of these lesions.

Differentiation of Lymphoma from GBM and Metastases

The preoperative diagnosis of lymphoma is extremely important because it can avoid the use of extensive unnecessary surgery for tumor removal, limiting the surgical procedure to a smaller biopsy for tissue characterization necessary for treatment decisions.[14-16] Recognizing lymphoma by imaging criteria is also essential because steroids are frequently administered in patients with brain tumor before a histologic diagnosis can be made, and there are doubts that steroid administration may affect the diagnostic yield of resection or stereotactic biopsy.[17,18] Pretreatment rCBV was found to be reduced in lymphomas compared with other lesions in our study. ROC, which evaluated the diagnostic performance of

rCBV and PSR, showed that max PSR had the best sensitivity and specificity in differentiating lymphoma from GBM and metastases.

There are only a few studies describing the PSR in lymphomas. In a study by Hartmann et al,[7] lymphomas exhibited a signal-intensity recovery curve that tended to cross the baseline, thereby implying that the PSR was higher than in gliomas. They attributed this to increased permeability and contrast enhancement in lymphomas due to endothelial disruption. This explanation does not match the phenomenologic observation of PSR by Cha et al[6], which implies that larger permeability leads to lower PSR. The exact cause of this high-signal-intensity recovery in lymphomas has so far not been clearly explained. However, it is known that in enhancing tumors, gadolinium diethylene triamine pentaacetic acid extravasates into the interstitial space of the lesion and causes complex T1 and T2* effects, which can alter the shape of the signal-intensity recovery curve. The T2* effects cause lower signal-intensity recovery while the T1 effects lead to higher signal-intensity recovery. When the T1 shortening effect, due to accumulation of contrast material in the interstitial space, dominates the T2* shortening effect, the signal intensity will increase and even exceed the baseline level.[19] These T1 and T2* effects of extravasated contrast also depend on the flip angle and TR used in the sequence.[20,21] In the study by Paulson and Schmanda,[22] this overshoot from baseline was explained as T1 effects of extravasated contrast. Effects of contrast agent preloading on rCBV measurements have been discussed previously. If a predose of contrast agent is given, even though the exact effect on PSR is not known, it is likely that T1 effects are cancelled or reduced while the T2* effects remain, resulting in a reduction in the postcontrast bolus baseline signal intensity and leading to lower PSR.[22-24]

Besides the permeability of capillaries, T2* and T1 effects of gadolinium in the EES are very complex, and other factors, like the type of tumor vascularity, accumulation rate, and quantity of contrast agent leakage in the interstitial space, may account for different T1 and T2* effects, which can lead to different PSRs. Due to the nature of PSR as a phenomenologic observation parameter, our study cannot differentiate multiple competing mechanisms behind the signal-intensity change during and after passage of the contrast agent. A clear understanding of the physics requires measurements of multiple relevant parameters and complete theoretic analysis, which is beyond the scope of this work.

Ultrastructural and histopathologic studies of the capillary architecture have shown that lymphomas are different from gliomas and metastases, with a complete absence of neoangiogenesis in the lymphomas.[25] There is also a difference in cellularity and structure of EES in these tumors. The hypercellular tumors like lymphoma with smaller extravascular space might have faster recovery. Due to different histopathologic ultrastructures in lymphomas, the contrast accumulation might be slow and T1 shortening and T2* shortening effects are not apparent during the first pass. Only after the first pass, does the T1 shortening effect overwhelm the T2* shortening effect, but not in GBM and metastases, which may lead to a higher percentage of signal-intensity recovery.[8] The higher percentage recovery may also depend on rate of blood flow in the tumor, and possibly the lesions with higher flow or arteriovenous shunt surgery might have a higher recovery. So far no definitive explanation is available for overshooting in lymphomas, but due to their compact cellularity and the different type of vasculature in lymphoma, the various physiologic factors, such as blood flow, blood volume, vascular permeability, and leakage space and the interplay between these factors, may alter the signal intensity in a complex way, leading to high PSR.

Differentiation of Metastases from GBM and Lymphoma

A solitary metastatic lesion commonly presents as an enhancing mass lesion and can be the first manifestation of a systemic malignancy.[26] It is very difficult to differentiate solitary metastases from other enhancing lesions on contrast-enhanced MR imaging. In our study, the max rCBV of an enhancing lesion was found not be a good parameter in differentiating metastases from GBM and lymphoma with an A_z of 0.5341 (Fig 3*B*). Min PSR and mean PSR yielded the best ROC characteristics and very high classification accuracy. This conformed to prior reports that found a significant difference in average signal-intensity height recovery, which was lower in metastases than in gliomas.[6]

Ultrastructural studies of GBM microvasculature have shown that it is composed of closely packed newly formed capillary buds and lined by hyperplastic endothelial cells that are partly invested by pericytes, and they may also retain some aspects of BBB architecture. On the other hand, capillary ultrastructure of metastases resembles the capillaries of the primary tumor, which has been shown in electron microscopy.[27] Thus, the absence of BBB in metastases results in a higher permeability and renders them far more susceptible to leakage.

The rCBV in the peritumoral region has been found to be higher in gliomas than in metastases due to the infiltrative nature of glioma and neoangiogenesis in the perienhancing region.[28] Our study also showed low rCBV and signal-intensity recovery in the perienhancing region of metastases compared with GBM and lymphoma. Similar findings showing mean and min perienhancing PSR to be better than perienhancing rCBV in the differentiation of metastases from GBM have been reported by Cha et al.[6]

The low-signal-intensity recovery in metastases has been attributed to a larger degree of alteration in capillary permeability. The T2* effects from markedly decreased intravascular contrast agent concentration and increased volume of distribution result in an increase in effective compartment size during the first pass, and it, in turn, alters the signal intensity in a complex way, leading to lower PSR in metastases. This type of lack of signal-intensity recovery or very low percentage of signal-intensity recovery can also be seen in extra-axial lesions due to the absence of a BBB. The reduction in PSR has also been used in the grading of gliomas and in differentiating recurrent metastases or glioma from radiation necrosis.[29-31] As mentioned above, the PSR is not completely understood but is most likely related to a number of factors, including compact EES, fast cerebral flow, and differences in capillary leakiness. It would be interesting to study the compact EES as a cause of overshooting and correlate the apparent diffusion coefficient with the PSR in various brain lesions such as lymphomas, because the apparent diffusion coefficient could serve as a very rough estimate of EES. The high PSR may also relate to leaky

components within a lesion; hence, measurements of the slope of signal-intensity recovery could also be important in future studies to help explain the physiologic basis of PSR.

Limitations

Several limitations exist in this study as a retrospective analysis. There may be an effect of steroid treatment on the perfusion parameters, and the patients in our study were treated with corticosteroids as clinically indicated. Some technical limitations exist as well. For instance, the presence of hemorrhage or susceptibility artifacts may render errors in the calculation of rCBV or signal-intensity recovery. Also, as described earlier, various perfusion parameters like PSR and rCBV described in this study can be affected by the MR imaging—acquisition protocol. We used a very strict and consistent imaging protocol for all tumors studied, including TR, TE, field strength, spatial resolution, flip angle, and type and dose of contrast agent administered. In this study, no preload dose of contrast agent was given because it allowed the signal intensity—time curve to better manifest itself and the PSR to be calculated. A few cases of metastases are without biopsy and were considered as metastases on the basis of a primary neoplasm elsewhere. The results reported in this study are observations made by using this protocol and these image processing methods in a relatively small number of patients with GBM, lymphoma, and metastases.

Conclusions

PSR calculated from signal-intensity curves obtained in T2*-weighted DSC measurements appears to be a simplified hemodynamic parameter that is clinically meaningful and effective in eliciting distinctive characteristics, which may help in differentiating lymphoma, metastases, and GBM. The PSR in other enhancing lesions of the brain should be evaluated in future studies. We recommend undertaking prospective studies and further effort to study the physiologic basis of PSR and to standardize the technique for its broader clinical applications.

Acknowledgements

The authors express sincere thanks to Dr. Hongmei Yang, PhD assistant professor, and Tao Lu, PhD student, Department of Biostatistics and Computational Biology, University of Rochester, for providing statistical help. The authors are also grateful to Linda Knutsson, PhD, and Oliver Thilmann, PhD, who were instrumental in the development of the LUPE software at Lund University and kindly gave us access to this software for evaluation of our MR perfusion examination.

References

1. Calli C, Kitis O, Yunten N, et al. **Perfusion and diffusion MR imaging in enhancing malignant cerebral tumors.** *Eur J Radiol* 2006;58:394–403
2. Weber MA, Zoubaa S, Schlieter M, et al. **Diagnostic performance of spectroscopic and perfusion MRI for distinction of brain tumors.** *Neurology* 2006;66:1899–906
3. Le Bihan D, Douek P, Argyropoulou M, et al. **Diffusion and perfusion magnetic resonance imaging in brain tumors.** *Top Magn Reson Imaging* 1993;5:25–31
4. Aronen HJ, Gazit IE, Louis DN, et al. **Cerebral blood volume maps of gliomas: comparison of tumor grade and histologic findings.** *Radiology* 1994;191:41–51
5. Sugahara TM, Korogi Y, Shigematsu Y, et al. **Perfusion-sensitive MRI of cerebral lymphomas: a preliminary report.** *J Comput Assist Tomogr* 1999;23:232–37
6. Cha S, Lupo JM, Chen MH, et al. **Differentiation of glioblastoma multiforme and single brain metastasis by peak height and percentage of signal intensity recovery derived from dynamic susceptibility-weighted contrast-enhanced perfusion MR imaging.** *AJNR Am J Neuroradiol* 2007;28:1078–84
7. Hartmann M, Heiland S, Harting I, et al. **Distinguishing of primary cerebral lymphoma from high-grade glioma with perfusion-weighted magnetic resonance imaging.** *Neurosci Lett* 2003;338:119–22
8. Liao W, Liu Y, Wang X, et al. **Differentiation of primary central nervous system lymphoma and high-grade glioma with dynamic susceptibility contrast-enhanced perfusion magnetic resonance imaging.** *Acta Radiol* 2008;50:2217–25
9. Haselhorst R, Kappos L, Bilecen D, et al. **Dynamic susceptibility contrast MR imaging of plaque development in multiple sclerosis: application of an extended blood-brain barrier leakage correction.** *J Magn Reson Imaging* 2000;11:495–505
10. Wetzel SG, Cha S, Johnson G, et al. **Relative cerebral blood volume measurements in intracranial mass lesions: interobserver and intraobserver reproducibility study.** *Radiology* 2002;224:797–803
11. Tello R, Crewson PE. **Hypothesis testing II: means.** *Radiology* 2003;227:1–4. Epub 2003 Feb 28
12. Wesseling P, Ruiter DJ, Burger PC. **Angiogenesis in brain tumors; pathobiological and clinical aspects.** *J Neurooncol* 1997;32:253–65
13. Jinnouchi T, Shibata S, Fukushima M, et al. **Ultrastructure of capillary permeability in human brain tumor. Part 6. Metastatic brain tumor with brain edema** [in Japanese]. *No Shinkei Geka* 1988;16:563–68
14. Haldorsen IS, Espeland A, Larsen JL, et al. **Diagnostic delay in primary central nervous system lymphoma.** *Acta Oncol* 2005;44:728–34
15. Roman-Goldstein SM, Goldman DL, Howieson J, et al. **MR of primary CNS lymphoma in immunologically normal patients.** *AJNR Am J Neuroradiol* 1992;13:1207–13
16. Kuker W, Nagele T, Korfel A, et al. **Primary central nervous system lymphomas (PCNSL): MRI features at presentation in 100 patients.** *J Neurooncol* 2005;72:169–77
17. Buhring U, Herrlinger U, Krings T, et al. **MRI features of primary central nervous system lymphomas at presentation.** *Neurology* 2001;57:393
18. Porter B, Giannini C, Kaufmann T, et al. **Primary central nervous system lymphoma can be histologically diagnosed after previously corticosteroid use: a pilot study to determine whether corticosteroids prevent the diagnosis of primary central nervous system lymphoma.** *Ann Neurol* 2008;63:662–67
19. Hakyemez B, Yildirim N, Erdogan, C, et al. **Meningiomas with conventional MRI findings resembling intraaxial tumors: can perfusion-weighted MRI be helpful in differentiation?** *Neuroradiology* 2006;48:695–702. Epub 2006 Aug 1
20. Boxerman JL, Schmainda KM, Weisskoff RM. **Relative cerebral blood volume maps corrected for contrast agent extravasation significantly correlate with glioma tumor grade, whereas uncorrected maps do not.** *AJNR Am J Neuroradiol* 2006;27:859–67
21. Uematsu H, Maeda M, Sadato N, et al. **Blood volume of gliomas determined by double-echo dynamic perfusion-weighted MR imaging: a preliminary study.** *AJNR Am J Neuroradiol* 2001;22:1915–19
22. Paulson ES, Schmainda KM. **Comparison of dynamic susceptibility-weighted contrast-enhanced MR methods: recommendations for measuring relative cerebral blood volume in brain tumors.** *Radiology* 2008;249:601–13
23. Levin JM, Wald LL, Kaufman MJ, et al. **T1 effects in sequential dynamic susceptibility contrast experiments.** *J Magn Reson* 1998;130:292–95
24. Runge VM, Kirsch JE, Wells JW, et al. **Repeat cerebral blood volume assessment with first-pass MR imaging.** *J Magn Reson Imaging* 1994;4:457–61
25. Kleihues P, Burger PC, Scheithauer BW. *Histological Typing of Tumours of the Central Nervous System.* Berlin, Germany; Springer-Verlag; 1999
26. Schiff D. **Single brain metastasis.** *Curr Treat Options Neurol* 2001;3:89–99
27. Long DM. **Capillary ultrastructure in human metastatic brain tumors.** *J Neurosurg* 1979;51:53–58
28. Law M, Cha S, Knopp EA, et al. **High-grade gliomas and solitary metastases: differentiation by using perfusion and proton spectroscopic MR imaging.** *Radiology* 2002;222:715–21
29. Lupo JM, Cha S, Chang SM, et al. **Dynamic susceptibility-weighted perfusion imaging of high-grade gliomas: characterization of spatial heterogeneity.** *AJNR Am J Neuroradiol* 2005;26:1446–54
30. Barajas RF, Chang JS, Sneed PK, et al. **Distinguishing recurrent intra-axial metastatic tumor from radiation necrosis following gamma knife radiosurgery using dynamic susceptibility-weighted contrast-enhanced perfusion MR imaging.** *AJNR Am J Neuroradiol* 2009;30:367–72. Epub 2008 Nov 20
31. Barajas RF Jr, Chang JS, Segal MR, et al. **Differentiation of recurrent glioblastoma multiforme from radiation necrosis after external beam radiation therapy with dynamic susceptibility-weighted contrast-enhanced perfusion MR imaging.** *Radiology* 2009;253:486–96